LANGMUIR

pubs.acs.org/Langmuir Article

Perspective of Tribological Mechanisms for α-Alkene Molecules with Different Chain Lengths from Interface Behavior

Xiaolong Liu, Zhiwen Zheng, Juhua Xiang, Hanwei Wang, Haizhong Wang, Dapeng Feng,* Dan Qiao,* and Hansheng Li

Cite This: https://doi.org/10.1021/acs.langmuir.4c03592 Read Online

ACCESS | Metrics & More | Article Recommendations

ABSTRACT: Three α-alkene lubricants, differentiated by chain length, were selected as model compounds to investigate the influence of chain length on tribological properties. The novelty of this study lies in setting chain length as the sole variable to explore its impact on surface and adsorption energy. Based on the above findings, the study provides a unique explanation of the intrinsic relationship between chain length and tribological performance. The tribological properties of the three α-alkenes were compared, and subsequent characterization methods elucidated the wear mechanisms and explored tribochemical reactions. The study employed the Owens−Wendt−Rabel−Kaelble (OWRK) method and density functional theory (DFT) to investigate each compound's surface energy and adsorption energy. Experimental results revealed that the average friction coefficients (abridged as COF) for 1-decene, 1-tetradecene, and 1-octadecene decreased sequentially to 0.125, 0.099, and 0.075, respectively. The wear volume of 1-tetradecene decreased by 53.2% and that of 1-octadecene decreased by 64.0% compared to 1-decene. This can be attributed to the simultaneous enhancement of the surface energy and adsorption energy with increasing chain length. On the one hand, the increase in surface energy facilitates tribochemical reactions positively influencing the formation of tribofilms. On the other hand, the increase in adsorption energy enhances the adsorption of lubricants on the substrate surface. The synergy of these two effects allows 1-octadecene and 1-tetradecene (long-chain α-alkenes) to exhibit superior tribological performance compared to that of 1-decene (short-chain α-alkenes). Ultimately, this study offers unique insights into understanding lubrication mechanisms.

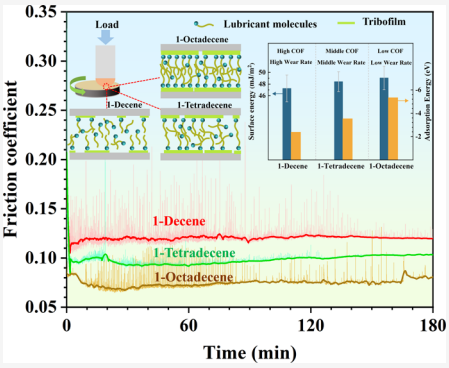

■ INTRODUCTION

In mechanical engineering and industrial production, the energy losses and equipment damage caused by friction are staggering,[1−3] making the development of lubrication technology key to ensuring the performance and efficiency of machinery.[3] Poly α-olefins (PAOs) synthetic base oils, prepared through the oligomerization of one or more linear α-alkenes in the presence of catalysts, represent a high-performance lubricating oil, gaining extensive utilization across a range of precision machinery equipment and greatly mitigating friction and wear.[4,5] As a significant class of organic compounds, α-alkenes have always been the raw material for the synthesis of PAOs.[6−8] The feedstocks for producing low-viscosity PAOs are primarily C_8−C_{12} linear α-alkenes with 1-decene being the main component, while longer chain α-alkenes are used to synthesize higher viscosity PAOs.[9] It is evident that the chain length of α-alkenes significantly impacts the properties of lubricants and thus their tribological properties. The length of the lubricant molecular chain is directly related to its viscosity,[10] and changes in viscosity can lead to alterations in the COF, wear mechanisms, and oil film thickness.[11,12] Recently, the tribological behavior of α-alkenes with different chain lengths on different substrates has been investigated by molecular simulation and friction tests, and some results have been obtained.

Summers[13] discovered through molecular dynamics simulations that the mechanism by which the in-plane arrangement of monolayer chains controls monolayer wear is achieved by promoting increased chain-to-chain contact between monolayers. Increasing the length of the monolayer chains can reduce the influence of substrate nonideality on degradation behavior, with C10 and C12 monolayers exhibiting considerably greater stability than C6 monolayers through an enhanced dispersion network. Erdemir et al.[14] employed *ab initio* molecular dynamics (AIMD) and reactive molecular dynamics (RMD) simulations to model the tribological chemistry of α-alkene (pentene) on copper surfaces within

Received: September 11, 2024
Revised: November 18, 2024
Accepted: November 18, 2024

PAOs, discovering that the pentene in PAOs facilitated the formation of a carbon-based solid lubricant film through dissociative extraction from themselves and this solid lubricant film plays an important role in improving lubrication performance. Li et al.[15] utilized RMD simulations to investigate the effect of linear α-alkenes of varying chain lengths in PAOs on the frictional behavior of a-C films. The experiments revealed that the synergistic action of thermal and shear effects led to the severe dissociation of α-alkene molecules at different parts of the C−C backbone. These show that the long-chain α-alkene lubricants are more prone to breakage on a-C surfaces under high friction forces, reducing the intact numbers of C_5H_{10}, C_8H_{16}, and $C_{12}H_{24}$ molecules by 58, 60, and 70%, respectively.

In systems such as liquid films, engine oils, and ionic liquids, changes in the chain lengths of the constituents will clearly alter their properties, as well as tribological performance. For instance, Jiménez et al.[16] investigated the influence of alkyl chain length and anion type on the lubricating ability in room-temperature ionic liquids. The results revealed that maintaining a consistent anion and extending the normal alkyl chain length (from n = 2 to 6 or 8) could reduce tribo-corrosion. Zhang et al.[17] conducted molecular dynamics (MD) simulations to study the frictional characteristics of six mixed alkane liquid films with different chain lengths between gold substrates, finding that the addition of short-chain alkane molecules, such as the n-hexane/dodecane mixed film exhibited the highest COF. This is attributed to the fact that short-chain molecules could decrease the density of the solid-like layer, causing the film transition from a solid-like state to a liquid state, and this transition in the film state increases friction. Mandal[18] demonstrated that additives with longer aliphatic chains exhibited stronger surface protective properties and lower COF in paraffin oil by comparing additives synthesized with different aliphatic chain lengths. Cyriac[19] employed a neutron reflectometer (NR) to study the influence of varying carbon chain lengths of organic friction modifiers (OFMs) on film formation, finding that long-chain and linear structured OFMs exhibited lower COF and wear, which is attributed to the fact that films formed by OFMs with longer chains is more effective at withstanding shear forces. The results of Booth et al.[20] showed that the tribological properties of monolayers depended on the surface groups, chain lengths, and head groups of the adsorbates, in which n-alkanethiolate monolayers with a chain length of 12 were irreparably damaged by a single pass of the probe under a force of 9.8 mN, whereas monolayers with longer chain lengths were more stable under the shear force of the probe and also exhibited better tribological properties, which was because increasing chain length improves the cushioning properties of the monolayers.

Computational simulations and tribological tests have both demonstrated that the chain length of lubricants or additives can significantly impact the manifestation of their tribological performance. The relationship between chain length and tribological properties requires further investigation, as this area has yet to be thoroughly explored. Herein, we must address a key question: what is the intrinsic relationship between chain length and the manifestation of its tribological performance? Additionally, another issue in the aforementioned research is that considering chain length variation as one of the factors inevitably leads to interference from other factors, such as base oils and additives, which prevents an accurate investigation of changes in lubrication performance caused solely by chain length variation. In this study, three α-alkenes of different chain lengths are used as model lubricants to uniquely study the impact of the chain length on lubrication performance. Friction experiments were conducted on three α-alkenes. The resulting wear scars and wear debris were characterized in detail, and the relationship between chain length and both adsorption and surface energies was also calculated. At the end of this article, a mechanism for the effect of chain length on the lubricating performance of lubricants was proposed. Ultimately, this study aspires to deepen the understanding of the relationship among chain length, tribological performance, and friction mechanisms.

■ EXPERIMENTAL SECTION

Materials. Three distinct α-alkenes, 1-decene, 1-tetradecene, and 1-octadecene, were acquired from Sinopharm Chemical Reagent Co., Ltd. and were utilized as is, without any additional processing. The molecular structures and photographs of these α-alkenes are illustrated in Figure 1. Any other solvents required for the experiment were procured from commercial sources.

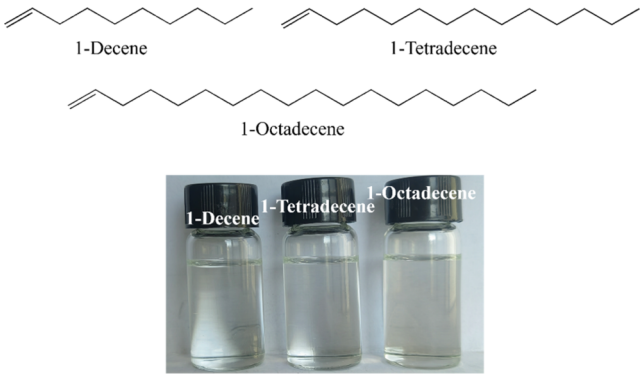

Figure 1. Structure and photograph of three α-alkenes.

Friction Test. For the friction testing, a ball-on-disc apparatus (MS-9000, Lanzhou Huahui Instrument Technology Co., Ltd.) was used, consisting of a stationary upper ball with a diameter of 10 mm and a mean roughness (R_a) of 0.10 μm, made of GCr15 steel with hardness ranging between 650 and 700 HV and a rotating lower disc with a diameter of 24 mm and a thickness of 7.9 mm, also made of GCr15 steel with the same hardness range. The schematic diagram of the friction pair is given in Figure 2. In the friction test, 10 mL of α-alkene was added to the oil box and three repetitive measurements were performed for each sample. The conditions of friction experiments were as follows: load of 200 N, speed of rotation of 300 rpm, radius of 5 mm, test duration of 180 min, and room temperature (RT).

Characterization. After the friction test, the α-alkene samples with debris were collected and centrifuged with a high-speed centrifuge to separate the lubricant and debris. The lower test disc and the centrifuged debris were cleaned twice with petroleum ether (PE) to remove the α-alkene attached to the surface. Wear debris and tribofilm were analyzed by a Raman spectroscope (HORIBA LabRam HR Evolution Confocal Raman microscope). The Raman system was utilized with the wavenumber range of 100−4000 cm^{-1} (laser = 532 nm, ND filter = 25%). X-ray photoelectron spectroscopy (XPS, Nexsa, Thermo Fisher Scientific Corporation) data were obtained on a spectrometer with Al Kα radiation as the exciting source. Micrographs were obtained via scanning electron microscopy (SEM, JSM-5601LV) coupled with energy dispersive X-ray spectroscopy (EDS), transmission electron microscopy (TEM, FEI Tecnai G2 F20), and high-resolution TEM (HRTEM).

Calculation of Wear Rate. The associated wear rate was determined utilizing eq 1:

https://doi.org/10.1021/acs.langmuir.4c03592
Langmuir XXXX, XXX, XXX−XXX

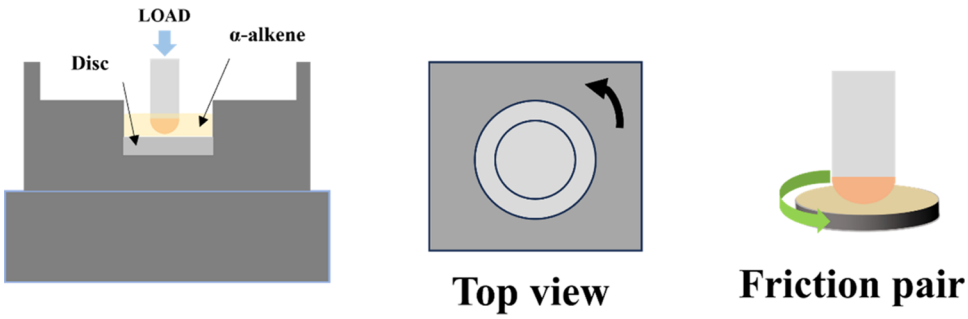

Figure 2. Experimental setup. Ring on disk tribometer. Test conditions: GCr15 steel versus GCr15 steel. α-Alkenes as a lubricant.

$$K = \frac{S \times L}{F \times l} \quad (1)$$

where K ($mm^3/N/m$) is the wear rate of the disc; F (N) and l (m) are the vertical force and moving length, respectively; L (mm) is the circumference of a circular wear scar; and S (mm^2) is the cross-sectional area of wear scar, which was photographed and calculated by a 3D profiler (VHX-6000).

Calculation of Adsorption Energy. Density functional theory (DFT) simulations were performed by using the Vienna Ab initio Simulation Package (VASP), employing plane-wave basis sets in conjunction with the projector augmented-wave technique. The treatment of exchange−correlation effects was facilitated through the utilization of the generalized gradient approximation (GGA), specifically with the Perdew−Burke−Ernzerhof (PBE) parametrization.[21−23] To account for van der Waals interactions, Grimme's DFT-D3 model corrections were integrated.[24] A vacuum space of approximately 18 Å was introduced to eliminate interactions across adjacent images. The energy cutoff parameter was determined to be 450 eV. For Brillouin-zone sampling, a Γ-centered Monkhorst−Pack scheme with a mesh size of 2 × 1 × 1 was adopted.[25] Structural optimizations continued until the maximal force on any atom was reduced below 0.02 eV/Å, with an energy convergence criterion of 10^{-5} eV being applied. Ultimately, adsorption energies ($E_{adsorption}$) were calculated according to the following equation: $E_{adsorption} = E_{lubricant/substrate}(E_{lubricant} + E_{substrate})$, where $E_{substrate}$ is the total energy of the isolated substrate, $E_{lubricant}$ is the energy of the lubricant molecule alone, and $E_{lubricant/substrate}$ is the energy of the combined stable lubricant/substrate system.

Surface Energy Test. The steel disc underwent an initial ultrasonic cleaning process in n-hexane for a duration of 5 min, following a period of drying and cooling to mitigate potential contamination. Then, 0.05 mL of three α-alkenes was individually applied onto the surface of each cleaned and cooled disk. Subsequently, the samples were left at RT for 2 h, during which an adsorption film developed on the disk surfaces. The cleaning of residual lubricant from the disc was accomplished by using n-hexane. Once dried, the disc was subjected to contact angle measurements to assess their surface properties based on test methods in the literature.[26]

To elucidate potential alterations on the surface, the surface energies of the disc, both prior to and following the formation of the adsorption film, were determined employing the Owens−Wendt−Rabel−Kaelble (OWRK) method (eq 2).[27−30] For this analysis, water and diiodomethane were chosen as the probing liquids, with their respective surface tensions presented in Table 1. The contact angles of these model liquids on the investigated surfaces were accurately measured using a video-based measuring device (DSA100, Krüss).

$$\gamma_L(1 + \cos\theta) = 2\left(\sqrt{\gamma_S^D \gamma_L^D} + \sqrt{\gamma_S^P \gamma_L^P}\right) \quad (2)$$

In the equation, γ_L represents the total surface energy of the liquid; θ denotes the contact angle of the liquid on the solid surface; γ_S^D signifies the surface energy of the solid's dispersive component; γ_L^D corresponds to the surface energy of the liquid's dispersive component; γ_S^P is the surface energy of the solid's polar component; and γ_L^P indicates the surface energy of the liquid's polar component.

Table 1. Surface Energy and Its Components of Model Liquids[27]

model liquids	polar component γ_L^P (mJ/m^2)	dispersive component γ_L^D (mJ/m^2)	total surface energy γ_L (mJ/m^2)
water	51.00	21.80	72.80
diiodomethane	0	50.80	50.80

Film Thickness Calculation. The utilization of the Hamrock−Dowson formulation in point contacts facilitates the estimation of the minimum lubrication film thickness under tribological stress for three classes of α-alkene.[31] The mathematical expression is delineated as (eq 3):

$$h_c = 2.69\frac{G^{0.53}U^{0.67}R}{W^{0.067}}(1 - 0.61\,e^{-0.73k}) \quad (3)$$

In this equation, h_c signifies the minimum film thickness, $G = \alpha E$, $U = \eta\upsilon/ER$, and $W = F/ER^2$, corresponding to the dimensionless parameters for the material's elastic modulus, rotational speed, and applied load, respectively. Within this context, α denotes the lubricant's pressure−viscosity coefficient, E represents the effective elastic modulus of the contacting bodies, and F is the applied load. k is the ellipticity factor, υ is the sliding linear velocity, which is calculated from the derivation of the following equation (eq 4), η is the viscosity of the lubricant at the RT, and n is the rotational speed.

$$V = \frac{2 \times \pi \times r \times n}{60 \times 1000} \quad (4)$$

The effective radius (R) of the steel ball is calculable through eq 5. In this context, D specifies the contact area of the steel ball, which can be determined from the diameter of the wear scar. The values of the parameters in eqs 3−5 are listed in Table 2.

$$R = \frac{ED^3}{6F} \quad (5)$$

RESULTS AND DISCUSSION

Friction Test. The COF of the steel−steel pair lubricated by three α-alkenes at 200 N is shown in Figure 3a. The average COF (Figure 3b, line graph) of 1-decene, 1-tetradecene, and 1-octadecene after running 180 min is 0.125, 0.099, and 0.075, respectively. The COF of 1-decene, 1-tetradecene, and 1-octadecene decrease sequentially, and its wear rate gradually decreases (Figure 3b, bar graph), which suggests that the chain length has an important effect on its tribological properties. In the friction tests described in this article, a high COF corresponds to a high wear rate, which is due to the fact that high COF causes thermal fatigue, oxidization, and detachment of the surface, thus increasing the wear rate.[32]

https://doi.org/10.1021/acs.langmuir.4c03592
Langmuir XXXX, XXX, XXX−XXX

Table 2. Values of the Parameters in Equations 3−5

parameter (unit)		value
α (GPa^{-1})	1-decene	1.4
	1-tetradecene	1.9
	1-octadecene	2.5
E (GPa)		208
F (N)		200
k		1
v (m/s)		0.157
η (Pa·s)	1-decene	7.59×10^{-4}
	1-tetradecene	1.66×10^{-3}
	1-octadecene	3.45×10^{-3}
n (rpm)		300
D (m^2)	1-decene	1.01×10^{-6}
	1-tetradecene	8.07×10^{-7}
	1-octadecene	5.30×10^{-7}

Meanwhile, the wear volume of 1-tetradecene decreases by 53.2% and that of 1-octadecene decreases by 64.0% compared to that of 1-decene, indicating that with the increase of the α-alkene chain length, its wear resistance increases.

The surface roughness of tribological pairs is a crucial factor influencing tribological performance.[33] To gain more profound insight into wear patterns, Figure 4 presents the three-dimensional (3D) topography and two-dimensional (2D) profile curves of wear tracks lubricated with the tested lubricants. It can be seen from 3D morphologies (Figure 4a−c) and the average 2D profiler (Figure 4d) that the wear scar with 1-decene as the lubricant has the deepest grooves and the largest wear rate, 1-tetradecene has shallow grooves and medium wear rate, and 1-octadecene has the lightest furrows and the smallest wear rate. In particular, the surface roughness of 1-decene, 1-tetradecene, and 1-octadecene decreases sequentially. Compared to 1-decene, the surface roughness of 1-tetradecene and 1-octadecene is reduced by 58 and 63.3%, respectively. This suggests that the chain length of the lubricant plays a crucial role in influencing its tribological performance.

Analysis of the Wear Scars and Wear Debris. *Raman Spectra of Wear Scars.* Figure 5 shows the Raman spectra of the blank steel as well as the abrasion marks of the steel block after the friction test. All of the surfaces of the steel blocks lubricated with α-alkenes showed obvious brownish-black wear scars, while there is no recognizable Raman peak on the blank steel surface. Further comparison with the reference iron oxides (Fe_2O_3 and Fe_3O_4) shows that the Raman spectra of the wear scars of the α-alkenes are more similar to those of Fe_3O_4, and this indicates that the friction process of the three α-alkenes is dominated by oxidative wear, which also explains the sharp fluctuation of their COF.[34] In addition, in Figure 5b$_1$,c$_1$,d$_1$, Raman absorption occurs at 2914 cm^{-1}, which is caused by the absorption of hydrogenated carbon present in the tribofilm.[34]

SEM and EDS Analysis of Wear Scars. In order to understand the lubrication mechanism, the wear scars were analyzed by using SEM (Figure 6) and EDS (Figure 7). As shown in Figure 6a,a1 (enlargement of Figure 6), it can be seen that the surface of the steel block with 1-decene has obvious furrows after the friction test. Evidently, the sliding surfaces have sustained significant damage with distinct metal deformation and pitting due to fatigue spalling on the worn surfaces. The wear characteristics are indicative of a composite mode of wear, where adhesive wear coexists with fatigue wear. In contrast, 1-tetradecene (Figure 6b) and 1-octadecene (Figure 6c), which have smaller wear rates after friction, show slight wear and further magnified observation of their surfaces (Figure 6b1,c1). Specifically, the worn surface of 1-tetradecene does not exhibit metal deformation or spalling but features broad scratches and furrows, which are characteristic of an abrasive wear mechanism. Similarly, the wear surface of 1-octadecene also shows slight furrowing; however, the broad scratches are absent and the surface becomes smoother, indicating that its wear mechanism is also attributed to abrasive wear. The above results show that the antiwear performance of α-alkenes increases with the chain length.

The EDS test results, as shown in Figure 7, indicate that the primary constituents identified on the surfaces of wear marks are C, O, and Fe. Notably, the concentrations of C and O in wear scars escalate sequentially with 1-decene, 1-tetradecene, and 1-octadecene, while Fe content diminishes progressively. This trend suggests that the content of C and O elements on the surface of the wear scar is enhanced with the elongation of the α-alkenes chain, and this may be attributed to the varying frictional chemical reactivity of α-alkenes. Consequently, these reactions facilitate the formation of a carbonaceous and oxide layer, augmenting the surface levels of C and O. The ensuing formation of carbonaceous and oxide films acts as a protective barrier, mitigating the metal surface's direct exposure and, thereby curtailing the direct abrasion and corrosion of metallic iron components, which results in a relative decrease in Fe content. Growing evidence[35−37] supports the notion that even pure hydrocarbons can generate carbon-based films on friction interfaces, suggesting that the frictional decomposition of α-

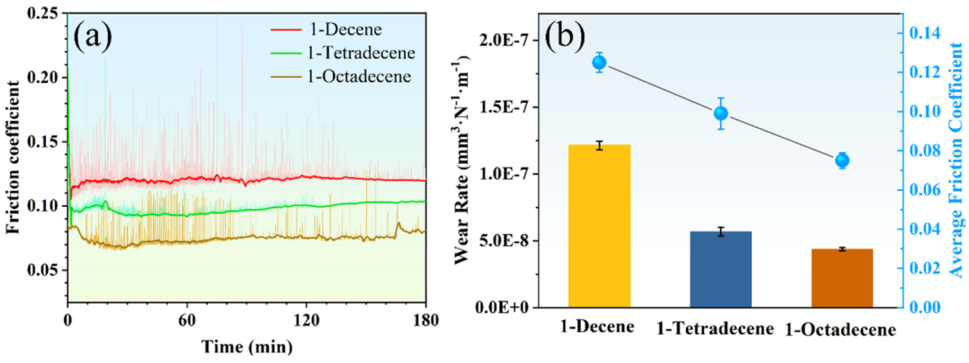

Figure 3. (a) Friction coefficient curves. (b) The wear rate of the steel disc lubricated by three α-alkenes.

https://doi.org/10.1021/acs.langmuir.4c03592
Langmuir XXXX, XXX, XXX−XXX

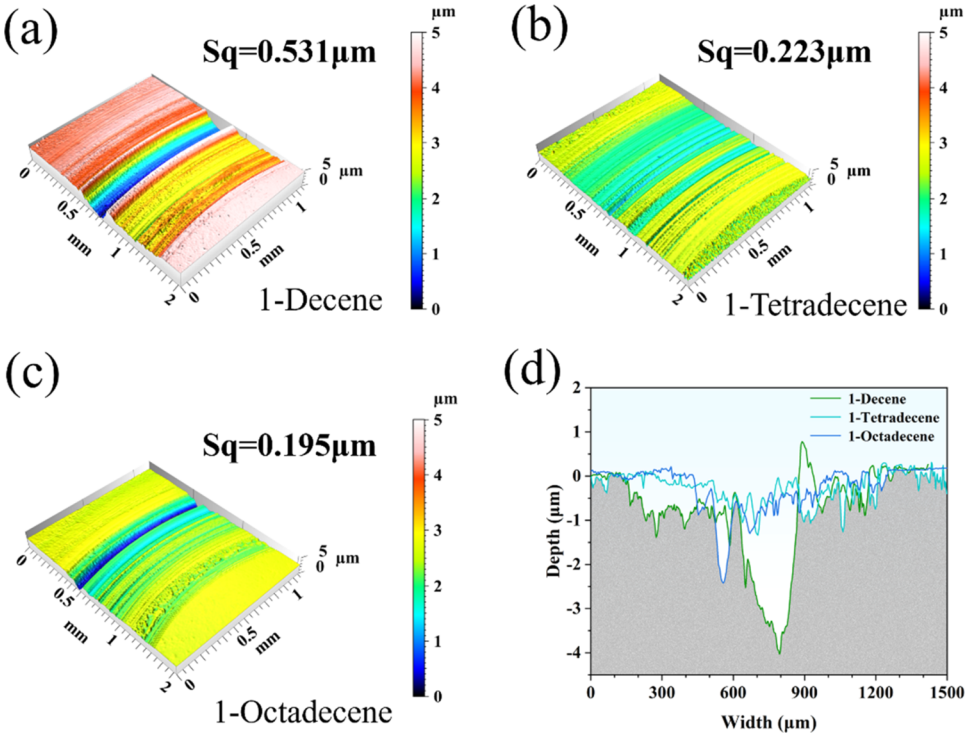

Figure 4. (a−c) 3D morphologies of wear scars lubricated by three α-alkenes, respectively. (d) The average 2D profile of three wear scars.

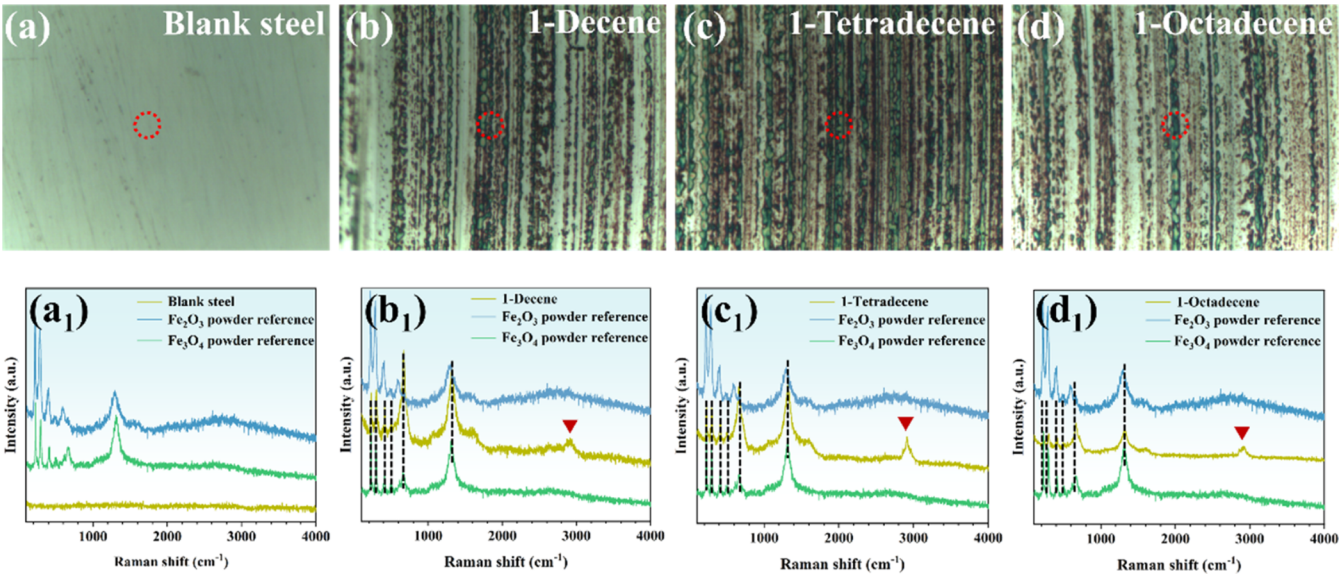

Figure 5. (a) Optical micrographs of a blank steel surface. Wear scars of steel surface lubricated by (b) 1-decene, (c) 1-tetradecene, and (d) 1-octadecene and their Raman spectra (a_1), (b_1), (c_1), (d_1), respectively.

alkenes, catalyzed by frictional heat and shear forces, may be a pivotal mechanism in this process.

XPS Spectra of Wear Scars. In order to better understand the friction of the surfaces during the rubbing process, XPS measurements of the three wear scars were performed to analyze the differences in the chemical compositions of the wear surfaces. Figure 8 shows the XPS spectra of C 1s, O 1s, and Fe 2p of the wear surfaces of the three α-alkenes. In the C 1s spectra of the three α-alkenes, 289.3 and 284.8 eV are attributed to C═O or COO− and adsorbed carbon,[38] indicating that a layer of carbon deposit is formed on the wear surface due to the decomposition of the lubricant during friction. The peaks appearing in 1-tetradecene at 286.3 eV and the peak appearing in 1-octadecene at 285.6 eV are both attributed to C−O,[38] whereas the peak appeared in the C 1s spectra of 1-decene at only 281.6 eV, which was attributed to Fe_3C, indicating the combination of C and Fe. However, the peak is absent in the spectra of 1-tetradecene and 1-octadecene. This absence may be attributed to the fact that these two α-alkenes are more actively involved in tribochemical reactions compared to 1-decene. As a result, they generate more carbon oxides that cover Fe_3C, making it undetectable by the instruments, and this is consistent with the results of the EDS analysis. The peak at 533.1 eV in the O 1s spectrum is

https://doi.org/10.1021/acs.langmuir.4c03592
Langmuir XXXX, XXX, XXX−XXX

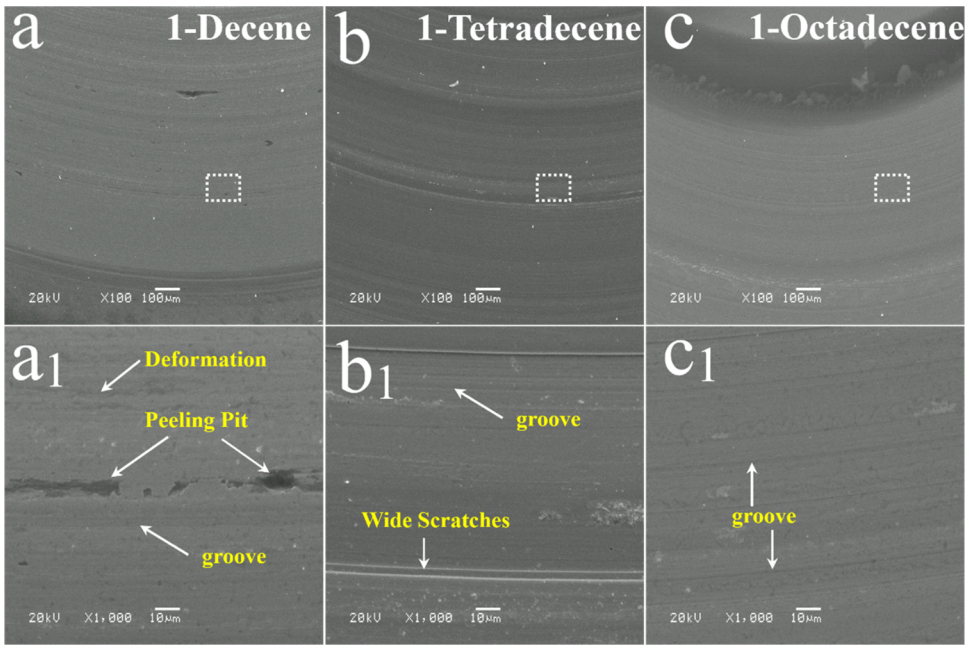

Figure 6. SEM images of wear marks of (a) 1-decene, (b) 1-tetradecene, and (c) 1-octadecene and enlarged images of (a_1) 1-decene, (b_1) 1-tetradecene, and (c_1) 1-octadecene.

assigned to FeOOH, while the peaks at 530.1 and 529.5 eV are attributed to Fe−O bonds,[39] combined with the Fe 2p peak near 725.6 eV, which corresponds to Fe_3O_4[40,41] this indicates that tribochemical reactions occurred on the wear surface due to direct contact of friction pairs, resulting in the formation of iron oxides and this is a primary factor in achieving excellent antiwear performance. Meanwhile, the peaks at 529.5 eV for 1-decene, 1-tetradecene, and 1-octadecene gradually intensify, suggesting an increase in iron oxides on the wear surface, leading to further degradation in wear resistance.[42] The binding energy at 532.1 eV in the O 1s spectrum is attributed to C−O bonds, considering other Fe 2p peaks located at approximately 713.2, 712.5, and 711.4 eV, and these can be identified as Fe_2O_3, Fe(OH)O, or FeO.[42,43]

Identification of Components for Wear Debris. TEM is frequently used to study the internal structure and composition of matter.[44,45] The analysis of the wear debris can reflect the tribofilm composition from another perspective. Therefore, the morphology of wear debris collected after the friction test was investigated by TEM. It can be seen intuitively from Figure 9a−c that the granularity of the wear debris generated by the friction of 1-decene, 1-tetradecene, and 1-octadecene decreases gradually, the distribution of the wear debris becomes finer and more uniform as the particle size decreases, and the smaller wear debris can help to form a more homogeneous and stable tribofilm on the sliding surfaces, which can effectively reduce the direct contact of metal and thus reduce the wear and improve the tribological performance, which is quite similar to the friction results described above. Typical lattice stripe spacings of 0.29 and 0.25 nm are seen in Figure 9a_1,b_1,c_1, which correspond to the crystal spacings of the (220) and (311) faces of Fe_3O_4, respectively.[40] This is corroborated by Raman's results. It is noteworthy that there are no lattice fringes of C in the image, which may be due to the fact that C produced by the friction reaction is amorphous carbon.

Analysis of Different Lubrication Properties of Three Different α-Alkenes. *Effect of Surface Energy on Tribological Properties.* The formation of an adsorption film by lubricant molecules on a steel substrate invariably modifies the substrate surface's physicochemical characteristics. To quantify the changes in surface energy following adsorption film formation, contact angle measurements were conducted (Figure 10a,b). The correlation between the surface energy of samples with an adsorption film at ambient temperature and the COF is depicted in Figure 10c. The surface energy of pristine steel (30.64 mJ/m^2) is observed to be lower than that of steel with an adsorption film. These findings indicate that the modeled lubricants are capable of forming adsorption films on the steel surface at room temperature. Analysis of frictional behavior reveals a negative correlation between the wear rate and COF with surface energy; namely, lubricant molecules exhibiting higher surface energy are associated with reduced wear rates and COF. In this study, the surface energies of 1-decene, 1-tetradecene, and 1-octadecene were determined to be 47.26, 48.42, and 49.06 mJ/m^2, respectively, with corresponding average COF and wear rates (mm^3/(N·m)) of 0.125, 0.099, and 0.075 and 1.213×10^{-7}, 5.676×10^{-8}, and 4.37×10^{-8}, respectively, aligning with the aforementioned relationship. Surface energy is elucidated as the excess energy of surface particles relative to those in the interior, with higher energy substances being more prone to instability.[46] Consequently, lubricant molecules in adsorption films with elevated surface energies are more susceptible to a tribochemistry reaction. Furthermore, wear rate and the COF are associated with the capacity of lubricant molecules to establish a film at the friction interface, suggesting that molecules with higher surface energies can therefore more easily form a protective film under frictional conditions and then mitigate direct contact between frictional surfaces and resulting in lower COF and wear rates.[34] It is imperative to acknowledge that while friction tests are subject to influences beyond surface energy, this investigation primarily elucidates

https://doi.org/10.1021/acs.langmuir.4c03592
Langmuir XXXX, XXX, XXX−XXX

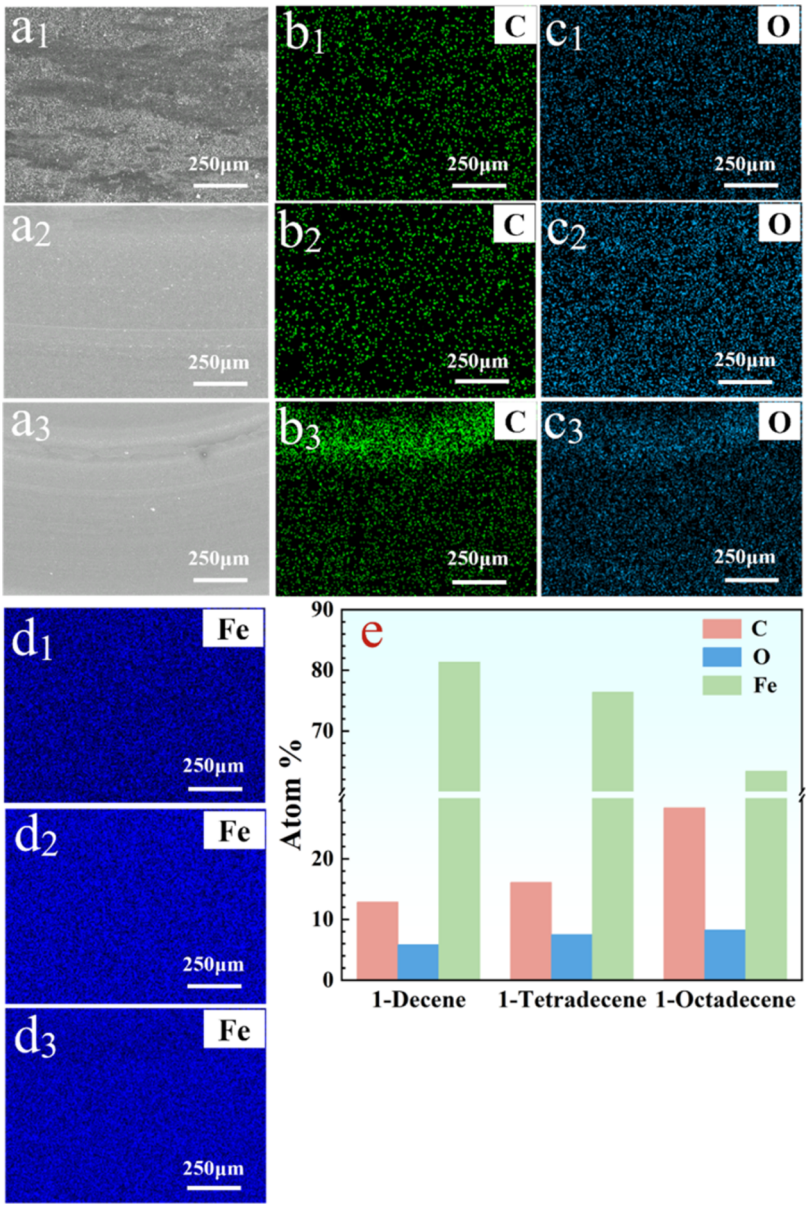

Figure 7. SEM images of 1-decene (a_1), 1-tetradecene (a_2), and 1-octadecene (a_3) and their DES images (b_1–d_1), (b_2–d_2) and (b_3–d_3), respectively. (e) Elemental content of wear marks.

the interplay between surface energy and the rates of wear and friction without delving into other contributory factors.

Effect of Adsorption Energy on Tribological Properties. As early as 1956, Bowden and Tabor proposed the theory of adhesive friction,[47] which states that the adsorption and film-forming properties of lubricants are important factors affecting the lubrication mechanism. In the friction process, before friction starts, the first step is the physical adsorption of the lubricant on the surface of the friction partner, and the size of the adsorption energy reflects the lubricant film-forming properties, thus directly affecting its lubricating properties.[48,49] Therefore, the study of the adsorption behavior of three α-alkene molecules with different chain lengths on steel substrates is of guiding significance for understanding the differences in their lubricating properties.

DFT calculations were employed to determine the adsorption energies of α-alkene molecules on the steel surface, as shown in Figure 11a. The adsorption energies for 1-decene, 1-tetradecene, and 1-octadecene are negative, indicating spontaneous adsorption, and the chain length of the α-alkenes markedly influences their adsorption energy. It is observed that an increase in the α-alkene chain length leads to an increase in the adsorption energy. This trend is attributed to the presence of additional carbon atoms and extended carbon chains in longer α-alkene molecules, which enhance the potential for interactions with the substrate. As depicted in Figure 11b, a higher adsorption energy correlates with a lower COF. The adsorption energy is computed by the difference between the total energy of the system postadsorption and the sum of the individual energies prior to adsorption. A greater adsorption energy signifies a more stable adsorption configuration, facilitating the adherence of lubricant molecules to the substrate surface. During relative motion, these lubricants can establish a film on the metal surface, anchoring at the head (C═C), with the flexible long alkyl chains extending along the direction of motion. Interactions between the long-chain tails

https://doi.org/10.1021/acs.langmuir.4c03592
Langmuir XXXX, XXX, XXX−XXX

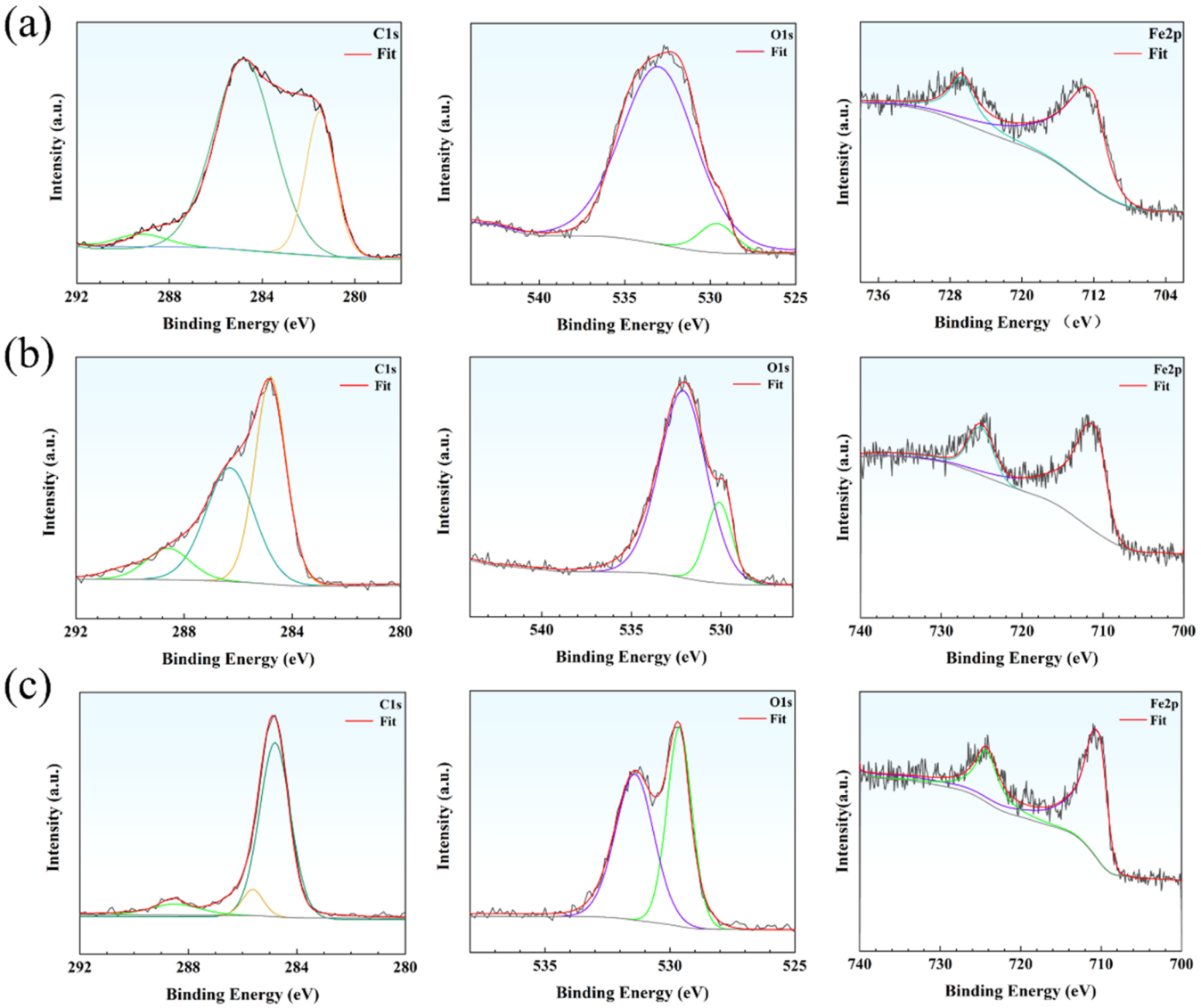

Figure 8. XPS of the wear scars on the steel−steel counterpart lubricated by (a) 1-decene, (b) 1-tetradecene, and (c) 1-octadecene.

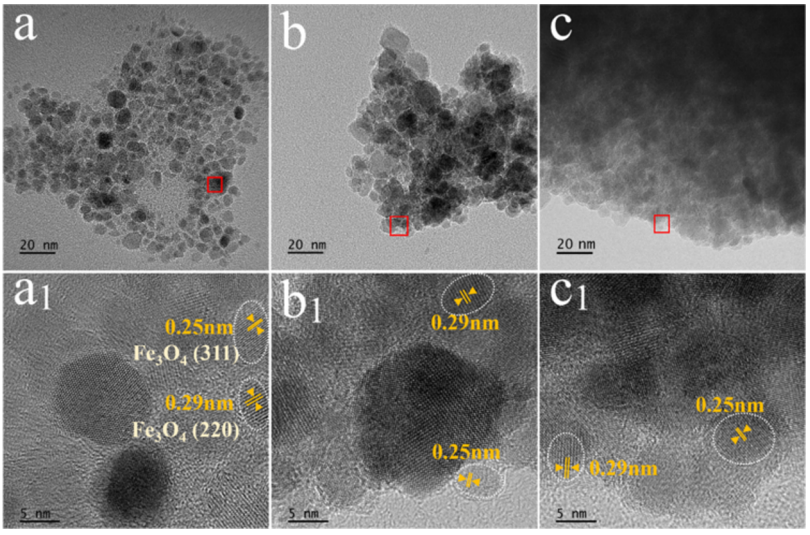

Figure 9. TEM images of wear debris of (a) 1-decene, (b) 1-tetradecene, and (c) 1-octadecene and their HRTEM image of wear debris (a_1), (b_1), and (c_1), respectively.

https://doi.org/10.1021/acs.langmuir.4c03592
Langmuir XXXX, XXX, XXX−XXX

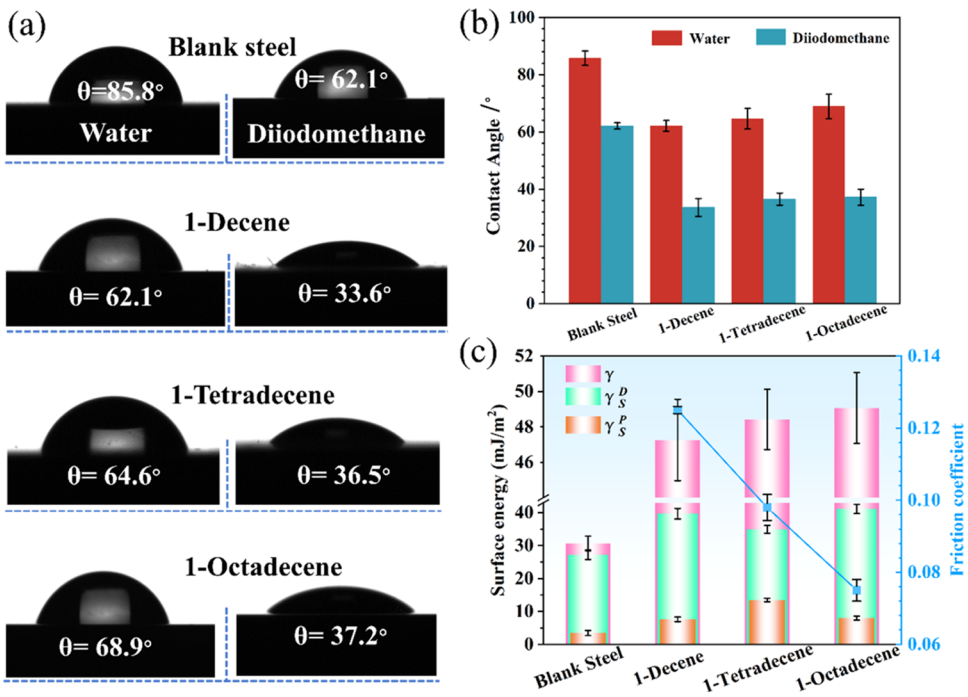

Figure 10. (a) Images of contact angles of model liquids (water and diiodomethane) on three α-alkenes liquid film surfaces, (b) histogram of contact angle of blank steel and α-alkenes, and (c) surface energy and corresponding COF of α-alkene molecules on the steel surface.

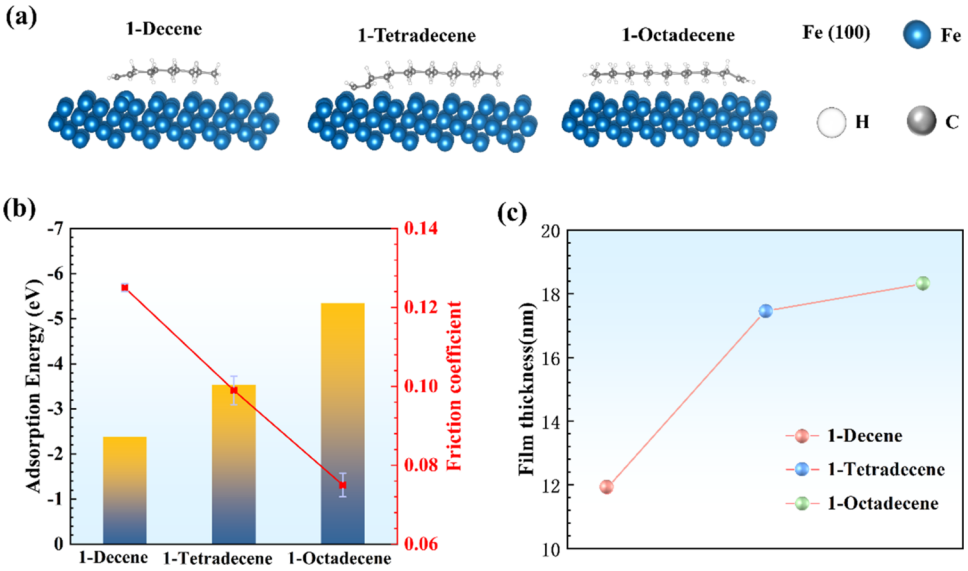

Figure 11. (a) Model lubricant molecules and Fe substrate employed in DFT calculations, (b) adsorption energies and COF (RT, 200 N, 300 rpm, 180 min) of three kinds of α-alkene molecules on the steel surface, and (c) tribofilm thicknesses of α-alkenes under friction conditions calculated using the Hamrock−Dowson theory.

of the adsorbed lubricant, primarily due to van der Waals forces, result in a densely packed adsorption layer.[50−52]

This adsorption layer reduces friction at the interface due to the collective strength of van der Waals forces, forming a film with remarkable durability capable of enduring considerable mechanical loads. Under the simultaneous action of load and shear stress, the incompressible adsorbed layer is predisposed to slip, culminating in the diminution of both frictional and adsorptive forces. Thus, molecules with enhanced adsorption energies exhibit a greater propensity to bond to the substrate and establish a stable adsorbed layer, resulting in a concomitant reduction in the COF.[53−55]

Film Thickness Calculation. Differences in the adsorption energies of α-alkenes inevitably influence their adsorption behaviors on substrate surfaces, ultimately resulting in variations in the thicknesses of the α-alkene adsorption films. To investigate the differences in the minimum film thicknesses of three types of α-alkenes under identical friction conditions, the Hamrock−Dowson model was applied to ascertain the minimal film thicknesses of three α-alkenes under specified frictional conditions, with the results exhibited in Figure 11c. This delineation shows a progressive increase in the film thicknesses for 1-decene, 1-tetradecene, and 1-octadecene, corroborating the previously inferred relationship that links the

https://doi.org/10.1021/acs.langmuir.4c03592
Langmuir XXXX, XXX, XXX−XXX

augmenting chain length of α-alkenes with enhanced adsorption energy. Consequently, under identical frictional circumstances, α-alkenes with a longer chain length demonstrate an increased tendency to adsorb to the substrate surface. This phenomenon leads to the formation of a thicker adsorption layer with longer chain α-alkenes for the same duration.

DISCUSSION

In this research, the influence of chain length on the tribological characteristics of 1-decene, 1-tetradecene, and 1-octadecene was investigated. It was observed that as the chain length increased (from 10 to 14 and 18), the average COF progressively diminished (from 0.125 to 0.099 and 0.075) and the wear rate also showed a significant decreasing trend. EDS results disclosed that the amounts of C and O elements in the wear scars of 1-decene, 1-tetradecene, and 1-octadecene increased in succession, suggesting that the extent of the tribochemical reaction involving the three α-alkenes also escalated. The C in the α-alkenes ultimately contributed to C detected in the wear scars. The thickness of the tribofilm of three α-alkenes increased sequentially, and this rise was positively associated with the decrease in the COF and wear rate. These findings imply that an increase in chain length is advantageous for improving the tribological performance of α-alkenes. Contact angle measurements and DFT calculations indicated that the surface energy and adsorption energy of the three α-alkenes showed an increasing tendency.

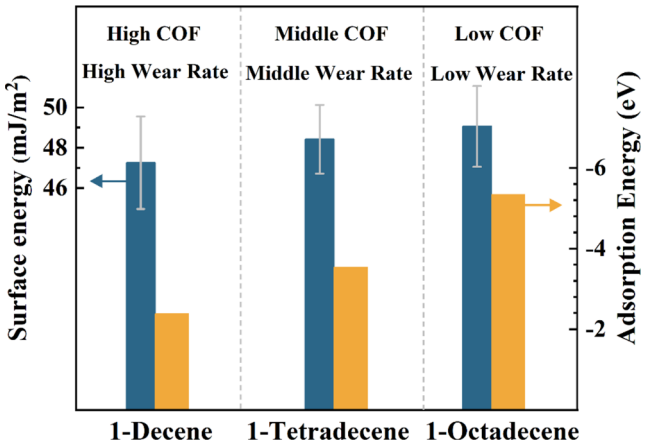

Figure 12. Relationship between adsorption energy and surface energy of α-alkene molecules on steel surfaces based on the coefficient of friction and wear rate.

The varying surface energy and adsorption energy endow α-alkenes with distinct tribological properties. Long-chain α-alkenes, characterized by high surface energy and high adsorption energy, benefit from the synergistic interaction of these two factors, resulting in superior tribological performance compared to short-chain α-alkenes, as elucidated in Figure 12.

Based on the analysis of experimental results and relevant literature reports, the mechanisms of tribological performance of different chain length α-alkene molecules have been summarized, as depicted in Figure 13. The variance in chain lengths endows the α-alkene molecules with distinct adsorption energies and surface energies. Prior to the onset of friction, α-alkenes on the sliding interface form bonds of varying strengths with the steel substrate, with long-chain α-alkenes possessing greater surface energies and higher adsorption energies more readily adsorbing onto the steel surface and forming a thin film. Once friction commences under the action of load and shear forces, the adsorption layer will inevitably be disrupted. However, long-chain α-alkenes with higher adsorption energies can readsorb onto the steel substrate surface more swiftly, repairing the damaged layer in a timely manner and maintaining a relatively intact adsorption layer (Figure 13c). Conversely, shorter-chain α-alkenes, with lower adsorption energies, engage in weaker interactions with the steel substrate and an inability to repair the layer damaged by shearing promptly in time (Figure 13a,b), resulting in a consistently higher COF throughout the process.

In conclusion, this review elucidates the differing tribological properties of α-alkenes with varying chain lengths by analyzing their surface and adsorption energies, which provides novel insight into lubrication mechanisms of lubricants.

CONCLUSIONS

In this study, we evaluated the tribological properties of α-alkenes with varying chain lengths and analyzed the composition of their wear scars and debris. We explored the

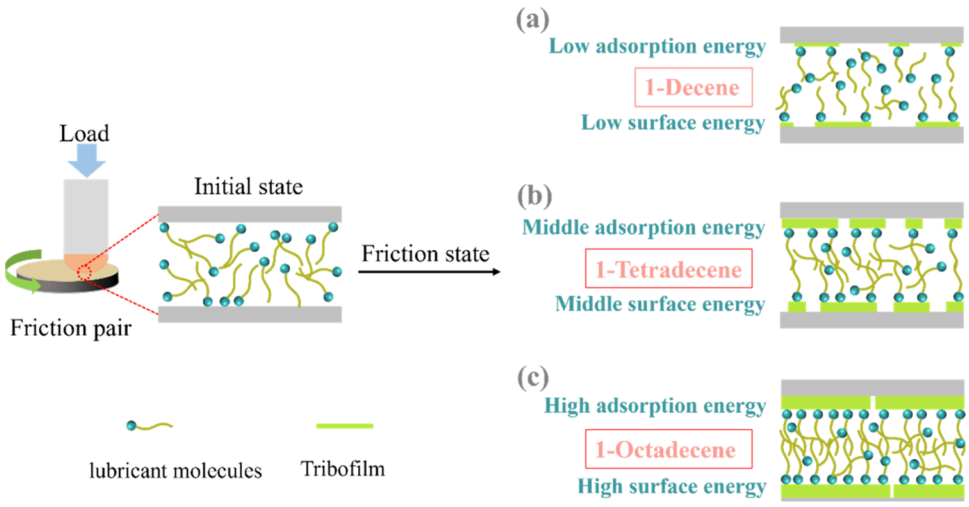

Figure 13. Mechanism of the chain length effect on the tribological properties of (a) 1-decene, (b) 1-tetradecene, and (c) 1-octadecene.

https://doi.org/10.1021/acs.langmuir.4c03592
Langmuir XXXX, XXX, XXX−XXX

intrinsic relationship between the α-alkene chain length and their tribological behavior. Compared to 1-decene (C_{10}), 1-tetradecene (C_{14}) and 1-octadecene (C_{18}) demonstrated reductions in the COF by 20.8 and 40.0%, respectively, and decreases in wear rate by 53.2 and 64.0%, respectively, indicating that within this experimental scope, long-chain α-alkenes exhibit superior tribological performance compared to their short-chain counterparts. Subsequent Raman, TEM, EDS, and XPS analyses confirmed that the friction-derived products from α-alkenes of varying chain lengths primarily consist of Fe_3O_4 and carbonaceous materials. Notably, the proportion of carbon and oxygen elements in the friction-derived products increases with the elongation of α-alkene chain length, facilitating the formation of films rich in carbonaceous and oxide materials. These films act as barriers, mitigating direct contact with the metal surface, thereby reducing wear, and this results in differing wear mechanisms. The morphological observations indicate that the wear mechanism with 1-decene as a lubricant is characterized as mixed wear, comprising both adhesive and fatigue wear. Conversely, when 1-tetradecene and 1-octadecene are used as lubricants, the wear mechanism is identified as abrasive wear.

Further investigation through surface energy and adsorption energy measurements revealed the intrinsic correlation between chain length and tribological properties, indicating a positive relationship between the α-alkene chain length and both surface and adsorption energies. Higher surface energy facilitates tribochemical film formation, while increased adsorption energy enhances the lubricant's ability to form a robust adsorptive layer on the substrate surface. The effect of these two factors enables long-chain α-alkenes (1-octadecene and 1-tetradecene) to exhibit better tribological properties than short-chain α-alkenes (1-decene). This research deepens the understanding of the interplay between chain length, tribological properties, and wear mechanisms.

■ AUTHOR INFORMATION

Corresponding Authors

Dapeng Feng − *State Key Laboratory of Solid Lubrication, Lanzhou Institute of Chemical Physics, Chinese Academy of Sciences, Lanzhou 730000, China;* orcid.org/0000-0002-8282-0242; Email: dpfeng@licp.cas.cn

Dan Qiao − *State Key Laboratory of Solid Lubrication, Lanzhou Institute of Chemical Physics, Chinese Academy of Sciences, Lanzhou 730000, China*; Email: ddqiao@licp.cas.cn

Authors

Xiaolong Liu − *State Key Laboratory of Solid Lubrication, Lanzhou Institute of Chemical Physics, Chinese Academy of Sciences, Lanzhou 730000, China; Center of Materials Science and Optoelectronics Engineering, University of Chinese Academy of Sciences, Beijing 100049, China*

Zhiwen Zheng − *State Key Laboratory of Solid Lubrication, Lanzhou Institute of Chemical Physics, Chinese Academy of Sciences, Lanzhou 730000, China*

Juhua Xiang − *State Key Laboratory of Solid Lubrication, Lanzhou Institute of Chemical Physics, Chinese Academy of Sciences, Lanzhou 730000, China; Center of Materials Science and Optoelectronics Engineering, University of Chinese Academy of Sciences, Beijing 100049, China*

Hanwei Wang − *State Key Laboratory of Solid Lubrication, Lanzhou Institute of Chemical Physics, Chinese Academy of Sciences, Lanzhou 730000, China; Center of Materials Science and Optoelectronics Engineering, University of Chinese Academy of Sciences, Beijing 100049, China*

Haizhong Wang − *State Key Laboratory of Solid Lubrication, Lanzhou Institute of Chemical Physics, Chinese Academy of Sciences, Lanzhou 730000, China*

Hansheng Li − *State Key Laboratory of Fluorinated Functional Membrane Materials, Dongyue Fluorosilicone Technology Group, Zibo 256400, China*

Complete contact information is available at: https://pubs.acs.org/10.1021/acs.langmuir.4c03592

Notes

The authors declare no competing financial interest.

■ ACKNOWLEDGMENTS

The authors are grateful for the financial support provided by the Youth Innovation Promotion Association CAS (2021422), the Shandong Natural Science Foundation Fluorosilicate Materials Mutual Fund (ZR2021LFG012), and the LICP Cooperation Foundation for Young Scholars LHJJ-20240104.

■ REFERENCES

(1) Yu, H.; Liu, X.; Zheng, Z.; Qiao, D.; Feng, D.; Gong, Z.; Dong, G. In Situ Graphene Formation Induced by Tribochemical Reaction for Sustainable Lubrication. *ACS Sustainable Chem. Eng.* **2023**, *11* (6), 2238−2248.

(2) Zheng, Z.; Liu, X.; Yu, H.; Chen, H.; Feng, D.; Qiao, D. Insight into Macroscale Superlubricity of Polyol Aqueous Solution Induced by Protic Ionic Liquid. *Friction* **2022**, *10* (12), 2000−2017.

(3) Gong, H.; Yu, C.; Zhang, L.; Xie, G.; Guo, D.; Luo, J. Intelligent Lubricating Materials: A Review. *Composites, Part B* **2020**, *202*, No. 108450.

(4) Hanifpour, A.; Bahri-Laleh, N.; Mohebbi, A.; Haghighi, M. N. Oligomerization of Higher α-Olefins to Poly (α-Olefins). *Iran. Polym. J.* **2022**, *31* (1), 107−126.

(5) Chen, Y.; Ji, M.; Zhang, F.; Li, J.; Pan, H.; Zhao, Y.; Zhang, Z.; Liu, L. Investigation of Tribological Behavior and Lubrication Mechanisms of Zinc Oxide under Poly α-Olefin Lubrication Enhanced by the Electric Field. *Langmuir* **2024**, *40* (13), 6741−6749.

(6) Zhao, Z.; Jiang, J.; Wang, F. An Economic Analysis of Twenty Light Olefin Production Pathways. *J. Energy Chem.* **2021**, *56*, 193−202.

(7) Sulima, S. I.; Bakun, V. G.; Chistyakova, N. S.; Larina, M. V.; Yakovenko, R. E.; Savost'yanov, A. P. Prospects for Technologies in the Production of Synthetic Base Stocks for Engine Oils (A Review). *Pet. Chem.* **2021**, *61*, 1178−1189.

(8) Rahbar, A.; Falcone, B.; Pareras, G.; Nekoomanesh, H. M.; Bahri, L. N.; Poater, A. Chain Walking in the $AlCl_3$ Catalyzed Cationic Polymerization of α-Olefins. *ChemPlusChem* **2023**, *88* (1), No. e202200432.

(9) Sadjadi, S.; Bahri-Laleh, N.; Nekoomanesh-Haghighi, M.; Ziaee, F.; Dehghani, S.; Shirbakht, S.; Rahbar, A.; Barough, M. S.; Mirmohammadi, S. A. Rationalizing Chain Microstructure in the Poly α-Olefins Synthesized by Cationic $AlCl_3/H_2O$ Catalytic System. *Int. J. Polym. Anal. Charact.* **2019**, *24* (6), 556−570.

(10) Risse, K.; Drusch, S. (Non)linear Interfacial Rheology of Tween, Brij and Span Stabilized Oil-Water Interfaces: Impact of the Molecular Structure of the Surfactant on the Interfacial Layer Stability. *Langmuir* **2024**, *40* (34), 18283−18296.

(11) Zhang, C.; Chen, J.; Liu, M.; Wang, F.; Zheng, Y.; Cheng, Y.; Liu, Z. Relationship Between Viscosity and Resistance of Oil Film: A New Way to Investigate the Controllable Friction Between Charged Interfaces Lubricated by Ionic Lubricating Oil. *Adv. Mater. Interfaces* **2022**, *9* (14), No. 2200229.

(12) Zheng, L.; Zhu, H.; Zhu, J.; Deng, Y. Effects of Oil Film Thickness and Viscosity on the Performance of Misaligned Journal Bearings with Couple Stress Lubricants. *Tribol. Int.* **2020**, *146*, No. 106229.

(13) Summers, A. Z.; Iacovella, C. R.; Billingsley, M. R.; Arnold, S. T.; Cummings, P. T.; McCabe, C. Influence of Surface Morphology on the Shear-Induced Wear of Alkylsilane Monolayers: Molecular Dynamics Study. *Langmuir* **2016**, *32* (10), 2348−2359.

(14) Erdemir, A.; Ramirez, G.; Eryilmaz, O. L.; Narayanan, B.; Liao, Y.; Kamath, G.; Sankaranarayanan, S. K. R. S. Carbon-Based Tribofilms from Lubricating Oils. *Nature* **2016**, *536* (7614), 67−71.

(15) Li, X.; Wang, A.; Lee, K. R. Tribo-Induced Structural Transformation and Lubricant Dissociation at Amorphous Carbon−Alpha Olefin Interface. *Adv. Theory Simul.* **2019**, *2* (2), No. 1800157.

(16) Jiménez, A.; Bermúdez, M. D.; Iglesias, P.; Carrión, F. J.; Martínez-Nicolás, G. 1-*N*-alkyl-3-Methylimidazolium Ionic Liquids as Neat Lubricants and Lubricant Additives in Steel-Aluminium Contacts. *Wear* **2006**, *260* (7−8), 766−782.

(17) Zhang, Z.-H.; Yu, X.; Li, H.; Han, K. Effect of Alkane Chain Length on Tribological Properties of Straight Chain Alkane Liquid Film. *Acta Phys. Sin.* **2019**, *68* (22), No. 228101.

(18) Mandal, S.; Murmu, M.; Sengupta, S.; Baranwal, R.; Hazra, A.; Hirani, H.; Banerjee, P. Effect of Molecular Chain Length on the Tribological Properties of Two Diazomethine Functionalised Molecules as Efficient Surface Protective Lubricant Additive: Experimental and *In Silico* Investigation. *J. Adhes. Sci. Technol.* **2023**, *37* (2), 213−239.

(19) Cyriac, F.; Tee, X. Y.; Poornachary, S. K.; Chow, P. S. Influence of Structural Factors on the Tribological Performance of Organic Friction Modifiers. *Friction* **2021**, *9* (2), 380−400.

(20) Booth, B. D.; Vilt, S. G.; McCabe, C.; Jennings, G. K. Tribology of Monolayer Films: Comparison Between N-Alkanethiols on Gold and N-Alkyl Trichlorosilanes on Silicon. *Langmuir* **2009**, *25* (17), 9995−10001.

(21) Kresse, G.; Furthmüller, J. Efficiency of *Ab-Initio* Total Energy Calculations for Metals and Semiconductors Using a Plane-Wave Basis Set. *Comput. Mater. Sci.* **1996**, *6* (1), 15−50.

(22) Kresse, G.; Furthmüller, J. Efficient Iterative Schemes for *Ab Initio* Total-Energy Calculations Using a Plane-Wave Basis Set. *Phys. Rev. B* **1996**, *54* (16), 11169−11186.

(23) Perdew, J. P.; Burke, K.; Emzerhof, M. Generalized Gradient Approximation Made Simple. *Phys. Rev. Lett.* **1996**, *77* (18), 3865−3868.

(24) Grimme, S.; Antony, J.; Ehrlich, S.; Krieg, H. A Consistent and Accurate *Ab Initio* Parametrization of Density Functional Dispersion Correction (DFT-D) for the 94 Elements H-Pu. *J. Chem. Phys.* **2010**, *132* (15), No. 154104.

(25) Pack, J. D.; Monkhorst, H. J. Special Points for Brillouin-Zone Integrations. *Phys. Rev. B* **1977**, *16* (4), 1748−1749.

(26) Goclawski, J.; Urbaniak-Domagala, W. In *The Method of Solid-Liquid Contact Angle Measurement Using the Images of Sessile Drops with Shadows on Substratum*, 2007 International Conference on Perspective Technologies and Methods in MEMS Design; IEEE, 2007; p 135.

(27) Kalin, M.; Polajnar, M. The Correlation Between the Surface Energy, the Contact Angle and the Spreading Parameter, and Their Relevance for the Wetting Behaviour of DLC with Lubricating Oils. *Tribol. Int.* **2013**, *66*, 225−233.

(28) Kus, M.; Kalin, M. Additive Chemical Structure and Its Effect on the Wetting Behaviour of Oil at 100 °C. *Appl. Surf. Sci.* **2020**, *506*, No. 145020.

(29) Han, Y.; Qiao, D.; Zhang, S.; Feng, D. Influence of Phosphate and Phosphonate Ionic Liquid Structures on Lubrication for Different Alloys (Mg, Al, Cu). *Tribol. Int.* **2017**, *114*, 469−477.

(30) Ba, Z.; Huang, G.; Qiao, D.; Feng, D. Experimental and Calculation Studies on the Relationship Between the Hygroscopic Behavior and Lubrication Properties of Ionic Liquids. *Appl. Surf. Sci.* **2020**, *529*, No. 147031.

(31) Hooke, C. J. The Elastohydrodynamic Lubrication of Heavily Loaded Point Contacts. *J. Mech. Eng. Sci.* **1980**, *22* (4), 183−187.

(32) Xu, X.; Xu, Z.; Sun, J.; Tang, G.; Su, F. In Situ Synthesizing Carbon-Based Film by Tribo-Induced Catalytic Degradation of Poly-α-Olefin Oil for Reducing Friction and Wear. *Langmuir* **2020**, *36* (35), 10555−10564.

(33) Ali, M. K. A.; Hou, X.; Li, Q.; Cai, Q.; Turkson, R. F.; Chen, B. Improving the Tribological Characteristics of Piston Ring Assembly in Automotive Engines Using Al_2O_3 and TiO_2 Nanomaterials as Nano-Lubricant Additives. *Tribol. Int.* **2016**, *103*, 540−554.

(34) Yu, H.; Chen, H.; Zheng, Z.; Qiao, D.; Feng, D.; Gong, Z.; Dong, G. Effect of Functional Groups on Tribological Properties of Lubricants and Mechanism Investigation. *Friction* **2023**, *11* (6), 911−926.

(35) Zhang, J.; Spikes, H. On the Mechanism of ZDDP Antiwear Film Formation. *Tribol. Lett.* **2016**, *63* (2), No. 24.

(36) Chen, Y.-N.; Ma, T.; Chen, Z.; Hu, Y.; Hu, W. Combined Effects of Structural Transformation and Hydrogen Passivation on the Frictional Behaviors of Hydrogenated Amorphous Carbon Films. *J. Phys. Chem. C* **2015**, *119* (28), 16148−16155.

(37) McClimon, J. B.; Hilbert, J.; Koshigan, K. D.; Fontaine, J.; Lukes, J. R.; Carpick, R. W. In Situ Growth and Characterization of Lubricious Carbon-Based Films Using Colloidal Probe Microscopy. *Tribol. Lett.* **2023**, *71* (2), No. 39.

(38) Yu, H.; Chen, H.; Zheng, Z.; Ba, Z.; Qiao, D.; Feng, D.; Gong, Z.; Dong, G. Transformation Mechanism Between the Frictional Interface under Dioctyl Sebacate Lubrication. *Tribol. Int.* **2021**, *155*, No. 106745.

(39) Su, T.; Song, G.; Zheng, D.; Ju, C.; Zhao, Q. Facile Synthesis of Protic Ionic Liquids Hybrid for Improving Antiwear and Anti-corrosion Properties of Water-Glycol. *Tribol. Int.* **2021**, *153* (1), No. 106660.

(40) Ba, Z.; Han, Y.; Qiao, D.; Feng, D.; Huang, G. Composite Nanoparticles Based on Hydrotalcite as High Performance Lubricant Additives. *Ind. Eng. Chem. Res.* **2018**, *57* (45), 15225−15233.

(41) Huang, G.; Yu, Q.; Ma, Z.; Cai, M.; Liu, W. Probing the Lubricating Mechanism of Oil-Soluble Ionic Liquids Additives. *Tribol. Int.* **2017**, *107*, 152−162.

(42) Zheng, Z.; Liu, X.; Yu, H.; Feng, D.; Qiao, D. Natural Cholesterol-Derived Ionic Liquids Enhancing the Antiwear Property and Biodegradability of Mineral/Vegetable Oils. *ACS Sustainable Chem. Eng.* **2022**, *10* (47), 15574−15588.

(43) Han, Y.; Qiao, D.; Guo, Y.; Feng, D. Tribological Performance and Mechanism of Phosphonate Ionic Liquids as Additives in Two Hydrocarbon Oils. *Tribology* **2017**, *37* (1), 27−34.

(44) Han, Y.; Wang, L.; Cao, K.; Zhou, J.; Zhu, Y.; Hou, Y.; Lu, Y. *In Situ* TEM Characterization and Modulation for Phase Engineering of Nanomaterials. *Chem. Rev.* **2023**, *123* (24), 14119−14184.

(45) Hu, Z.; Fan, X.; Diao, D. A Review of *In-Situ* TEM Studies on the Mechanical and Tribological Behaviors of Carbon-Based Materials. *Lubricants* **2023**, *11* (5), No. 11050187.

(46) Marichev, V. Vague Concept of "Reversible Cleavage" in the Theory of the Surface Tension of Solids. *Surf. Sci.* **2009**, *603* (21), 3212−3214.

(47) Bowden, F.; Tabor, D. *The Friction and Lubrication of Solids*; Oxford University Press, 1956.

(48) Tang, H.; Sun, J.; He, J.; Wu, P. Research Progress of Interface Conditions and Tribological Reactions: A Review. *J. Ind. Eng. Chem.* **2021**, *94*, 105−121.

(49) Shaigan, N.; Neill, W. S.; Littlejohns, J.; Song, D.; Lafrance, S. Adsorption of Lubricity Improver Additives on Sliding Surfaces. *Tribol. Int.* **2020**, *141*, No. 105920.

(50) Kumar, D.; Singh, A.; Mishra, D. K. Role of Surfactant Head Group and Chain Length in Aqueous Lubrication: Steel-Steel Contact. *Proc. Inst. Mech. Eng., Part J* **2016**, *230* (8), 968−973.

(51) Quiroga, M. A. O.; Cabeza, G. F. Role of Van der Waals Forces in Graphene Adsorption over Pd, Pt, and Ni. *Braz. J. Phys.* **2013**, *43* (3), 126−129.

https://doi.org/10.1021/acs.langmuir.4c03592
Langmuir XXXX, XXX, XXX−XXX

(52) Davidson, J. E.; Hinchley, S. L.; Harris, S. G.; Parkin, A.; Parsons, S.; Tasker, P. A. Molecular Dynamics Simulations to Aid the Rational Design of Organic Friction Modifiers. *J. Mol. Graphics Modell.* **2006**, *25* (4), 495−506.
(53) Beltzer, M.; Jahanmir, S. Role of Dispersion Interactions Between Hydrocarbon Chains in Boundary Lubrication. *ASLE Trans.* **1987**, *30* (1), 47−54.
(54) Song, W.; Campen, S.; Shiel, H.; Gattinoni, C.; Zhang, J.; Wong, J. S. S. Position of Carbonyl Group Affects Tribological Performance of Ester Friction Modifiers. *ACS Appl. Mater. Interfaces* **2024**, *16* (16), 14252−14262.
(55) Marmorat, T.; Wijanarko, W.; Espallargas, N.; Khanmohammad, H. Effect of the Polar Head Type on the Surface Adsorption and Tribofilm Formation of Organic Friction Modifiers in Water-Based Lubricants. *Langmuir* **2024**, *40*, 7920−7932.

https://doi.org/10.1021/acs.langmuir.4c03592
Langmuir XXXX, XXX, XXX−XXX